Close-range hyperspectral spectroscopy reveals leaf water content dynamics

Junttila, Samuli

2022-08

Junttila , S , Hölttä , T , Saarinen , N , Kankare , V , Yrttimaa , T , Hyyppa , J & Vastaranta , M 2022 , ' Close-range hyperspectral spectroscopy reveals leaf water content dynamics ' , Remote Sensing of Environment , vol. 277 , 113071 . https://doi.org/10.1016/j.rse.2022.113071

http://hdl.handle.net/10138/345404
https://doi.org/10.1016/j.rse.2022.113071

Remote Sensing of Environment 277 (2022) 113071

Contents lists available at ScienceDirect

Remote Sensing of Environment

journal homepage: www.elsevier.com/locate/rse

Close-range hyperspectral spectroscopy reveals leaf water content dynamics

S. Junttila [a,*], T. Hölttä [b], N. Saarinen [a], V. Kankare [a], T. Yrttimaa [a], J. Hyyppä [c], M. Vastaranta [a]

[a] School of Forest Sciences, University of Eastern Finland, Joensuu 80101, Finland
[b] Department of Forest Sciences, University of Helsinki, Helsinki 00014, Finland
[c] Department of Remote Sensing and Photogrammetry, Finnish Geospatial Research Institute, National Land Survey of Finland (NLS), Masala, 02431, Finland

ARTICLE INFO

Edited by Jing M. Chen

Keywords:
Equivalent water thickness
Relative water content
Leaf mass per area
Hyperspectral imaging
Remote sensing
Leaf spectra
Shortwave infrared reflectance
Spectral prediction
Diurnal cycle

ABSTRACT

Water plays a crucial role in maintaining plant functionality and drives many ecophysiological processes. The distribution of water resources is in a continuous change due to global warming affecting the productivity of ecosystems around the globe, but there is a lack of non-destructive methods capable of continuous monitoring of plant and leaf water content that would help us in understanding the consequences of the redistribution of water. We studied the utilization of novel small hyperspectral sensors in the 1350–1650 nm and 2000–2450 nm spectral ranges in non-destructive estimation of leaf water content in laboratory and field conditions. We found that the sensors captured up to 96% of the variation in equivalent water thickness (EWT, g/m^2) and up to 90% of the variation in relative water content (RWC). Further tests were done with an indoor plant (*Dracaena marginate* Lem.) by continuously measuring leaf spectra while drought conditions developed, which revealed detailed diurnal dynamics of leaf water content. The laboratory findings were supported by field measurements, where repeated leaf spectra measurements were in fair agreement ($R^2 = 0.70$) with RWC and showed similar diurnal dynamics. The estimation of leaf mass per area (LMA) using leaf spectra was investigated as a pathway to improved RWC estimation, but no significant improvement was found. We conclude that close-range hyperspectral spectroscopy can provide a novel tool for continuous measurement of leaf water content at the single leaf level and help us to better understand plant responses to varying environmental conditions.

1. Introduction

Insights into the movement of water within plants, plant communities and ecosystems are crucial for understanding their responses to the environment. Measurement methods of leaf water content that can detect small differences that occur on diurnal or shorter time scales are needed to understand the interrelations of stomatal conductance, carbon exchange, water uptake and leaf water status (Hao et al., 2010). Knowledge on plant hydraulic traits and their variability is necessary for understanding the capabilities of plants in adjusting to a changing environment (Rosas et al., 2019). Leaf water content affects many plant physiological processes such as stomatal conductance, photosynthesis and growth, but there is a lack of methods that are capable of continuously monitoring leaf water content of single leaves or tree canopies, especially in the subtle ranges that occur on a diurnal basis. Stomatal control and leaf gas exchange have been modelled based on environmental conditions, such as vapour pressure deficit (VPD) and light, without explicitly considering the plant hydraulics and water status of the leaf (Dewar et al., 2018; Sperry et al., 2016). Recently it has become evident that considering these in addition to the environmental can deepen our understanding of leaf gas fluxes. Improved estimation and measurement methods of leaf water content can lead to better understanding and modelling of the relations between carbon exchange and the environment.

Leaf water content can be assessed using multiple metrics. The direct physical representation of the layer of water within a leaf is measured as equivalent water thickness (EWT) or the mass of water per leaf area. EWT is often used as a metric in remote sensing literature due to the direct physical relationship between leaf absorption and EWT (Feret et al., 2019). However, EWT does not directly translate into plant water status, which we often are interested in. Leaf water potential is probably the most widely used metric of plant water status and it is strongly related to the relative water content (RWC) of leaves (i.e., the amount of water in the leaf per the amount of water in the leaf in turgid state)

* Corresponding author at: School of Forest Sciences, University of Eastern Finland, Yliopistokatu 7, 80101 Joensuu, Finland.
E-mail address: samuli.junttila@uef.fi (S. Junttila).

https://doi.org/10.1016/j.rse.2022.113071
Received 25 August 2021; Received in revised form 14 April 2022; Accepted 29 April 2022
Available online 10 May 2022

(Bartlett et al., 2012; Rahimi et al., 2010). But due to the close relation between leaf spectra and EWT, remote sensing scientists have focused more on estimating EWT. However, the change in EWT can be linked to the change in RWC, which provides a possibility to estimate plant water status using leaf spectral reflectance (Browne et al., 2020).

Remote sensing scientists have been studying the estimation of leaf water content for decades using the changes in infrared reflectance caused by altered leaf water content (Ceccato et al., 2001; Cheng et al., 2011; Danson et al., 1992; Penuelas et al., 1993; Penuelas et al., 1997; Tucker, 1980). Various approaches and techniques have been used with different application perspectives and varying levels of success, for estimating leaf water content with wide ranging spatial scales, including terrestrial lidar (Elsherif et al., 2019a; Junttila et al., 2019; Junttila et al., 2021), imaging spectroscopy (Kotz et al., 2004), terahertz radiation spectroscopy (Browne et al., 2020) and microwave remote sensing (Konings et al., 2019). These studies however lack in providing practical solutions to estimating dynamic changes in leaf water content.

There are still many limiting factors with existing remote sensing methodologies in monitoring leaf water content from single trees several times a day. The limitation of passive spectroscopy is its dependence on external illumination, challenging the collection of dense time-series for assessing diurnal leaf water content dynamics. Active sensors such as terrestrial lidar can provide backscatter measurements any time of the day, but these devices have not been designed for spectral measurements and suffer from calibration issues (Junttila et al., 2019; Korpela, 2017). In addition, the temporal resolution of many of the developed approaches has been limited. Repetition rate of the measurements in addition to illumination conditions (especially when using passive imaging) limit the temporal coverage of airborne and satellite measurements, again hampering the measurement of diurnal leaf water content dynamics.

Stomatal control of transpiration is a sum of various different mechanisms. The stomata react e.g. to changes of water availability in the soil during drought in the time scale of hours or days (Tuzet et al., 2003). In addition, the stomata also react in the time scale of minutes to fast changes in environmental conditions around the leaves caused e.g. by fluctuating light due to sunflecks (Campany et al., 2016) and fast changes in VPD which are coupled to rapid changes in bulk leaf water content, leaf hydraulics and leaf water storage and release capacity (Schymanski et al., 2013), and also to very local changes in the water content of the guard cells of the stomata and the surrounding epidermal cell (Buckley, 2005). In each case, the water status of the leaf and stomatal conductance are tightly coupled through feedbacks. There has been a lack of methods that can accurately measure changes in leaf water content non-destructively with a temporal resolution in the range of minutes, that could enhance the understanding between leaf water dynamics and leaf gas exchange. Respectively, widely applied methods used to assess plant water status, such as destructive measurements of RWC and leaf water potential, are labour intensive, require destructive sampling and are practically impossible to conduct at short time intervals for a long period of time (e.g. Turner and Long (1980)). Novel leaf water content measurement methods with high temporal resolutions could greatly enhance our understanding of the relationships between vapour pressure deficit (VPD) and leaf water content and therefore plant drought tolerance.

Leaf reflectance in the shortwave infrared (SWIR) region (1300–2500 nm) is affected to a large extent by leaf structure and water content. EWT and leaf structure are the dominating traits in this region, but also leaf mass per area (LMA) contributes to the variation in leaf reflectance in the SWIR region (Feret et al., 2008; Yang et al., 2021), thus, complicating the retrieval of leaf water content from spectral measurements. Therefore, the effect of leaf structure and LMA should be minimized to achieve high accuracies in the retrieval of leaf water content (Feret et al., 2019). Geographically local and species-wise models that are developed to a limited range of leaf structural types and LMA could provide considerably higher accuracies in the estimation of leaf water content by reducing variation in reflectance induced by leaf structural traits. The estimation of LMA on the other hand could assist in the estimation of RWC, which is more closely linked to plant water status than EWT, because the water storage capacity of leaves depends on LMA (Garnier and Laurent, 1994). In addition to EWT and LMA, the leaf structure and organization of cells may induce considerable variation to SWIR reflectance even within species and can change throughout the growing season (Boren et al., 2019).

The advancement of sensor technology has recently enabled the construction of handheld spectrometers (Beć et al., 2020). Miniaturization and lower costs have opened up new avenues for scientific and practical applications using spectroscopy when the sensors are becoming more widely available both in research and business (Huck, 2021). Where a traditional spectrometer has required a backpack, the most recent sensors are the size of a matchbox and enable high temporal resolutions with continuous measurements of a single plant or a leaf, which are not possible using destructive sampling. In this study, we aimed to test if a small low-cost (under 2500 €) hyperspectral sensor could be used to monitor the diurnal dynamics of leaf water content, and potentially replace the use of destructive sampling methods in assessing leaf water content and plant water status.

The aim of the study was to evaluate the capabilities of low-cost hyperspectral spectroscopy in monitoring diurnal variation of leaf water content using destructive and in-situ measurements, and leaf reflectance simulation. We had the following research questions (RQ):

RQ 1. Can hyperspectral spectroscopy in the spectral ranges between 1350 nm and 1650 nm and 2000 nm and 2450 nm be used to monitor the diurnal variation in leaf water content?

RQ 2. What kind of predictive accuracy can be achieved in estimating leaf water content using low-cost hyperspectral spectroscopy?

RQ 3. Can the estimation of LMA lead to improved estimation of RWC?

These three research questions were investigated in three different empirical experiments to estimate the accuracy of the developed method and to cover short- and long-term monitoring of leaf water content in both field and laboratory conditions.

2. Material and methods

2.1. Outline of the conducted experiments

This study consists of three different empirical experiments and a leaf reflectance spectrum simulation. We first used the PROSPECT-D leaf reflectance model to investigate the effect of EWT, LMA and leaf structure (leaf structural parameter N) on leaf reflectance spectrum in the SWIR region (Féret et al., 2017). Then, we used experimental data collected in two experiments (see below) to investigate the interlinkages between EWT, RWC and LMA to examine if the retrieval of LMA could improve the estimation of RWC. The aim of the first experiment (Experiment 1) was to investigate the estimation accuracy of EWT, RWC and LMA using hyperspectral reflectance measurements in the SWIR region and determine suitable wavelengths for measuring these variables ($n = 44$). The aim of the second experiment (Experiment 2) was to investigate the capabilities of the investigated sensors in detecting diurnal variation in EWT and RWC through continuous measurement of leaf reflectance spectra for 20 days in a controlled environment ($n = 2$). The third experiment (Experiment 3) aimed at investigating the measurement of the diurnal leaf water cycle in field conditions using repeated leaf spectrum measurements (10 leaves measured seven times) and destructive sampling. A schematic figure of the experiment designs is presented in Fig. 1.

The first study was conducted using destructive sampling, thus, EWT, LMA and leaf structure (N parameter in PROSPECT-D leaf reflectance model) varied between each sample. In the last two experiments, time-series data of leaf reflectance was used to reduce the amount of variation

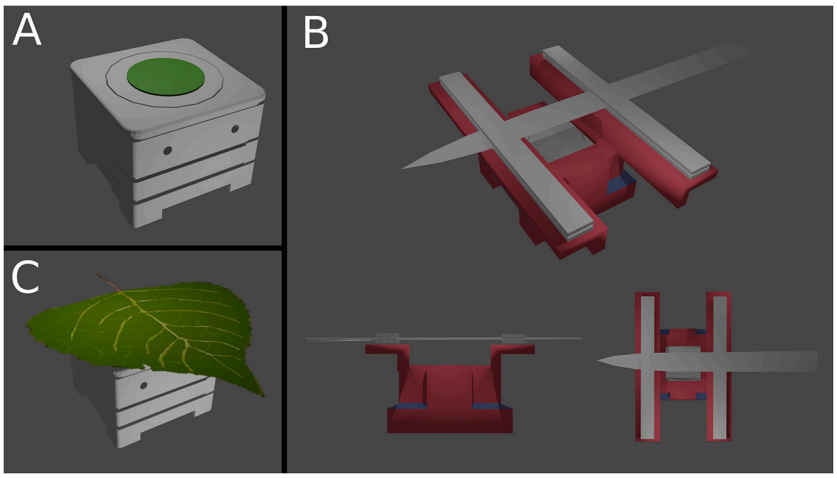

Fig. 1. Schematic representations of (A) experiment 1 with a leaf disc on top the NIRONE sensor, (B) experiment 2 with a leaf mounted on a sensor mount for continuous measurement, and (C) experiment 3 with a leaf on top of a NIRONE sensor (not detached).

caused by LMA and leaf structural parameter N on leaf reflectance spectrum and the estimation of leaf water dynamics.

2.2. Simulation of leaf spectra using PROSPECT-D

Leaf reflectance was simulated using PROSPECT-D leaf reflectance model to investigate the effect of leaf structural parameter N and leaf density expressed as LMA on leaf reflectance spectrum (Féret et al., 2017). PROSPECT is a leaf reflectance model that simulates directional-hemispherical reflectance and transmittance based on biophysical and biochemical variables in addition to leaf structural parameter N. Leaf pigment concentrations were neglected because our simulations were concentrated on exploring the effect of leaf water content and structure in the SWIR region, which is not affected by leaf pigments. The simulations were constrained by the ranges of LMA and EWT measured in the field experiment of this study (Experiment 3). Because the estimation of N parameter from spectrum was not possible due to the limited spectral range (Feret et al., 2008), we used a range between 1.8 and 2.5 that has been observed previously to occur within species (Boren et al., 2019).

2.3. Investigated hyperspectral sensors

We investigated two small sized hyperspectral sensors in leaf water content monitoring: NIRONE S1.7 (Spectral Engines, Espoo, Finland) and NIRONE S2.5. These sensors measure 1350–1650 nm region and 2000–2450 nm region, respectively. The sensors have two vacuum tungsten lamps that illuminate the target. The wavelengths can be programmed but the full width at half maximum is 13–17 nm for the S1.7 sensor and 18–28 nm for the S2.5 sensor. The detector in the sensors is a single element extended InGaAs type. Light enters the detector through a hole that is one millimeter in diameter. The viewing angle of the sensor is only 8 degrees; thus, resulting in a narrow measurement area when measuring at close-range. Signal-to-noise ratio is 11,000 for the S1.7 sensor and 1500 for the S2.5 sensor. The sensor dimensions are 25 × 25 × 17.5 mm and it weighs 15 g. The sensor parameters used in the measurements were a point average of 100 and a scan average of three. Examples of leaf spectra are shown in Fig. 2.

2.4. Experiment 1

The first experiment was conducted on the 26th of August 2020 in the Viikki campus area in Helsinki, Finland. Twigs of silver birch (*Betula pendula* Roth) were detached from a young silver birch tree (height: 3.5 m, diameter at breast height 3 cm) and put immediately under water for a re-cut to maintain water connectivity in the xylem. Leaves were then covered with aluminium foil and bagged with a plastic bag to allow full rehydration of the leaves for three hours. The twigs were then carried to the laboratory for further measurements.

We measured 21 leaves in total using 44 leaf discs cut from the leaves. A set of four fully hydrated leaves were detached from the branch and placed on the table for sampling. The leaves were sampled two to three times within 60 min with the aim of obtaining a continuous range of leaf water statuses. A leaf disc of 10 mm diameter was cut from a leaf, weighted and the leaf reflectance was measured from the abaxial side using NIRONE S1.7 and S2.5 sensors consequently (Fig. 1). The remaining leaf was left to dry for 30–60 min and an additional disc or

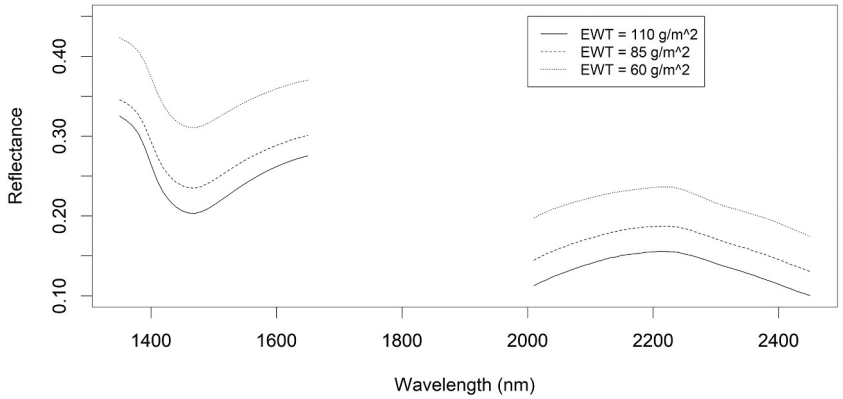

Fig. 2. Example of measured leaf spectra using NIRONE S1.7 and S2.5 with samples of varying equivalent water thickness (EWT, g/m^2).

two were cut during that time. We measured a total of 44 leaf discs, i.e. two discs per leaf were measured on average. The leaf discs were then merged under water for 12 h to allow full hydration and weighted to measure turgid weight. The leaf discs were then dried in 60 °C for 48 h until they reached a constant mass and the dry weight was measured (Mullan and Pietragalla, 2012). It should be noted that using leaf discs can be used as a uniform sampling technique for leaf segments but may induce overestimation of RWC (Arndt et al., 2015). However, as we focused on covering a wide range of RWC values to investigate which wavelengths are the most sensitive to water content, the oversaturation issue became insignificant. This approach also allowed us to reduce error arising from within leaf water content variation (that would have arisen from measuring entire leaves) by matching the water content measurements with the small footprint of the spectral measurements.

2.5. Leaf functional traits

Leaf functional traits EWT, RWC and LMA were measured in experiments 1 and 3 (Tables 1 & 2). EWT was measured by calculating the mass of water within a leaf disc (fresh weight – dry weight) and dividing that by the area of the leaf disc, expressed as g/m^2. RWC was calculated by dividing the mass of water within a leaf disc by the difference between turgid weight and dry weight, expressed as percentages. LMA was calculated by dividing dry weight by leaf area.

2.6. Experiment 2

The second experiment was conducted in laboratory conditions with a common monocot house plant: *Dracaena marginate* Lem. using three leaves. The plant consisted of two stems growing in the same pot with heights of 1.2 m and 0.5 m. The plant was subjected to natural light from a west facing window, but the plant was subjected to direct sunlight only a few hours per day. Three hyperspectral spectroscopy sensors were installed in the plant to continuously measure leaf reflectance: NIRONE S1.7 (1350–1650 nm) and NIRONE S2.5 (2000–2450 nm). Each sensor was mounted to measure a different leaf. The NIRONE S1.7 and S2.5 were measuring leaves of the taller stem. A custom 3D printed sensor mount was developed for this purpose, which kept the leaf and the sensor in place. Because the sensors generate heat, they were installed to measure at a 1.0 cm distance. The sensor mount design can be found from the supplementary files. After the installation of the sensors, the plant was left to adjust for three days.

The *D. marginate* was subjected to drought during the monitoring period by scheduling a sparse watering schedule. The plant was monitored from the 19th of March to the 8th of April and was watered twice during this period: on the 25th of March 1.0 l of water was given and on the 6th of April 0.5 l of water. The plant was well-watered before the start of the monitoring period.

We investigated how the leaf spectra changed during the time between the 26th of March and April 5th (the period without watering), during which drought slowly developed as the amount of water in the soil depleted. We used time from last watering (TLW) as a coarse proxy of leaf water content during the drought period to identify wavelengths capable of capturing variation in RWC. We note that there are limitations in the relationship between TLW and leaf water content, but it is well-known that leaf water content depletes as drought intensifies (Egilla et al., 2005; Li-Ping et al., 2006; White et al., 1996).

Table 1
The mean, minimum, maximum and standard deviation of equivalent water thickness (EWT) and relative water content (RWC) of the measured leaf disc samples ($n = 44$).

	Mean	Minimum	Maximum	Standard deviation
EWT (g/m^2)	85.5	54.7	114.6	16.5
RWC (%)	73.6	44.3	95.3	14.5
LMA (g/m^2)	68.3	57.3	78.9	5.6

Table 2
The mean, minimum, maximum and standard deviation of equivalent water thickness (EWT), relative water content (RWC) and leaf mass per area (LMA) of the measured leaf samples ($n = 21$).

	Mean	Minimum	Maximum	Standard deviation
EWT (g/m^2)	123.8	107.2	139.3	10.1
RWC (%)	93.9	90.5	96.1	2.5
LMA (g/m^2)	95.6	87.2	104.4	11.0

2.7. Experiment 3

Another experiment was conducted using repeated spectral measurements of 10 silver birch leaves between the 31st of August and the 1st of September 2020 in Hyytiälä Forest Research Station. The station is located at Juupajoki municipality in Southern Finland, where a station for measuring ecosystem-atmosphere relations (SMEAR II) is also located. The test forest site was a 58-year-old Scots pine (*Pinus sylvestris* L.) stand with admixtures of Norway spruce (*Picea abies* (L.) Karst.), rowan (*Sorbus aucuparia* L.), European aspen (*Populus tremula* L.), and common juniper (*Juniperus communis* L.). We monitored a mature silver birch (height: 18 m, diameter at breast height: 25 cm) for 22 h using NIRONE S1.7 and NIRONE S2.5 sensors and a linear displacement transducer dendrometer (G series spring Push, Vg/5/s, Solartron Inc., West Sussex, UK) at 1.5 m height to measure diurnal changes in xylem diameter. Ten healthy leaves were randomly selected from the canopy for repeated measurements using the NIRONE sensors. A marker was used to outline the measurement area to avoid the influence of within leaf variation of leaf properties on the measurement. A single measurement of each leaf was conducted at seven time points during the monitoring period representing different leaf water status stages based on the diameter of the tree xylem. In addition, three leaves were destructively sampled for the measurement of RWC, EWT and LMA at each time point using same methods as for experiment 1 (Table 2). The leaf area was measured using a flatbed scanner (Epson V300, Suwa, Japan) and image analysis.

2.8. Spectral features

Spectral features were calculated from the measured reflectance values to investigate the dependence between spectra and leaf water content metrics. The measurements of NIRONE sensors were combined for each leaf and a normalized ratio index (NRI) of each wavelength combination was calculated (Eq. (1)).

$$NRI = \frac{\gamma_1 - \gamma_2}{\gamma_1 + \gamma_2} \quad (1)$$

where γ_1 and γ_2 are the reflectance of each wavelength.

The spectral features included the mean measured reflectance of each wavelength and the NRI.

Daily metrics of leaf spectra were calculated in the drought experiment (Experiment 3) to describe the development of spectral features over time. The daily metrics were the mean and range of each spectral feature for each day during the monitoring period.

2.9. Statistical analysis

First, destructive leaf sample measurements of EWT, RWC and LMA from experiment 1 and 3 were combined to investigate the interrelations of the measured leaf functional traits and the capability of EWT and LMA in predicting variation in RWC. A subset of experiment 1 was used by including only samples with RWC above 85% to avoid the effect of the drying of leaves and to focus the analysis on a range of RWC values that can occur in a diurnal timeframe. We used Pearson's correlation

coefficient to investigate the correlation between EWT, RWC and LMA and linear regression modelling to investigate the capabilities of EWT and LMA in predicting RWC.

Then, we investigated leaf spectra and developed linear regression models between the spectral features and the leaf functional traits to investigate their relations and capability to explain variation in EWT, RWC and LMA, and to identify suitable wavelengths. Single spectral features were used as predictors of the leaf functional traits (referred to as direct approach in the text). We also explored the prediction accuracy of RWC using the best spectral predictors of EWT and LMA as an alternative approach for predicting RWC. The rationale for this approach was the strong theoretical foundation of the effects of EWT and LMA on leaf spectra (Feret et al., 2019).

In the second experiment, regression models were developed between TLW and daily metrics of spectral features to evaluate their capability in capturing changes in leaf water content over time during drought conditions and to identify prominent wavelengths for *D. marginate* (monocot vs. dicot silver birch). Then, a regression model was built using data from Experiment 1 and RWC was predicted for the monitoring period. Note that the regression model was built using data from silver birch and not *D. marginate*.

In the third experiment, the spectral features that were identified most prominent in Experiment 1 were used to test their predictive capabilities in field conditions. Mean of destructively measured RWC and spectral features of the 10 leaves were used to build regression models to estimate RWC. Two approaches for estimating RWC were tested: direct prediction of RWC using leaf spectra (direct approach) and prediction of RWC using the best spectral predictors of EWT and LMA (alternative approach).

We used coefficient of determination (R^2), root-mean-square-error (RMSE) and mean absolute error (MAE) to evaluate the goodness of the models in explaining variation in leaf water content using leave-one-out cross-validation. The top five of the spectral features for explaining the variation in leaf water content are depicted in the results for each experiment. All the statistical analyses were conducted using R software (R Core Team, 2013) and the hsdar package for convenient handling of spectral data (Lehnert et al., 2018).

3. Results

3.1. Simulation of leaf spectrum variation induced by leaf structure and water content

Simulation of leaf spectrum revealed differences in the amount of variance induced by leaf structural traits (N and LMA) and water content (EWT) (Fig. 3). The simulations showed that leaf structural parameter N causes the majority of the variation in reflectance in the SWIR region. EWT showed to induce more variation than LMA especially in the 1390–1500 nm and 1850–2100 nm wavelength regions. The amount of variance caused by EWT and LMA was nearly equal in the 1600–1800 nm and 2150–2350 nm wavelength regions.

3.2. Estimation of leaf water content and leaf mass per area using leaf spectra in the short-wave infrared region (Experiment 1)

Both investigated sensors showed high sensitivity to changes in leaf water content with increasing reflectance indicating decreasing leaf water content. Reflectance of every measured wavelength showed capable of estimating EWT with accuracies (RMSE) ranging between 5.91 g/m^2 and 9.48 g/m^2 (Table 3). NIRONE S2.5 with the spectral range of 2000–2450 nm showed more consistent prediction accuracies of both EWT and RWC compared to the 1350–1650 nm range. The most accurate models in estimating EWT were using wavelengths: 2020 nm, 2050 nm, 2010 nm, and 2030 nm. The most accurate models in estimating RWC were developed using wavelengths: 2010 nm, 2020 nm, 2000 nm, and 2040 nm. However, there were small differences (R^2 varied only 0.03 units) between wavelengths in the 2000–2450 nm domain in the estimation accuracy of both leaf water content metrics. Single wavelength features did not exhibit statistically significant relationships with LMA.

The regression models that utilized two wavelengths (i.e., normalized ratio indices) were superior in terms of explaining variation in both EWT and RWC (Table 4). The NRIs explained up to 96% and 93% of the variation in EWT using the 1350–1650 nm and 2000–2450 nm spectral regions, respectively (Fig. 4). Variation in RWC was explained up to 90% and 89% by the 2000–2450 nm and 1350–1650 nm spectral regions, respectively. The highest estimation accuracy of EWT was achieved with an NRI of 1390 nm and 1370 nm wavelengths providing an RMSE of

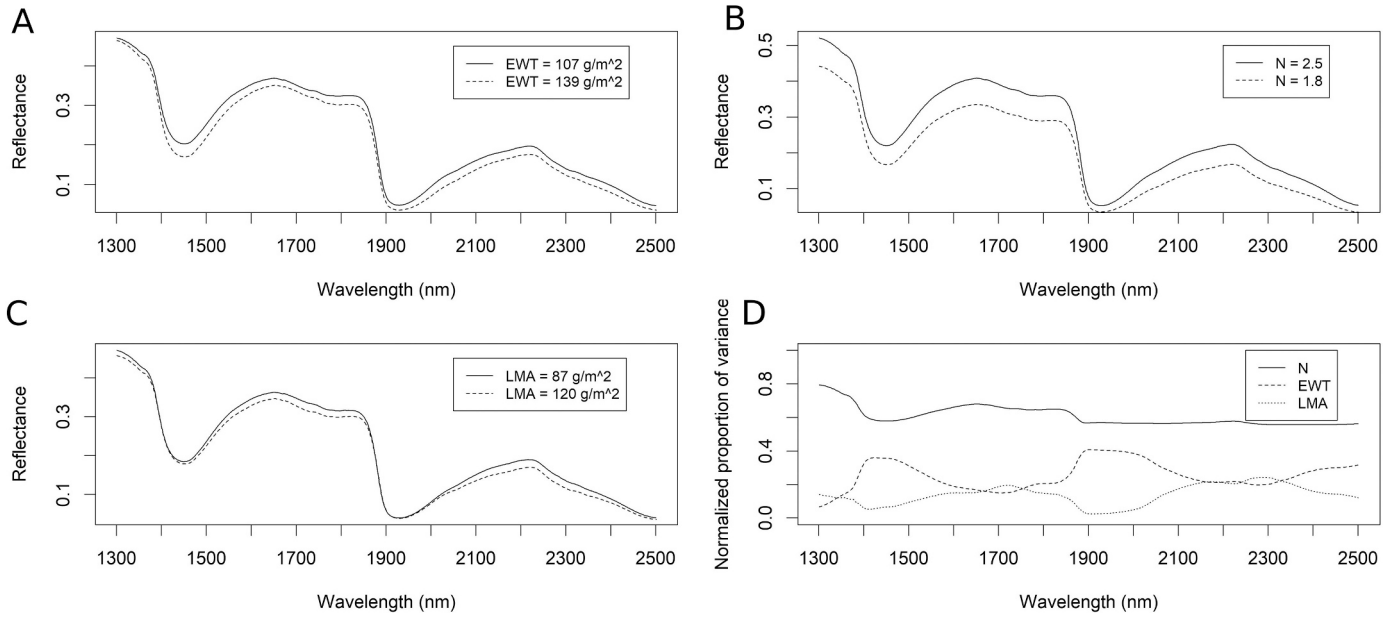

Fig. 3. Leaf reflectance spectrum simulated using PROSPECT-D. Other parameters were kept constant while A) equivalent water thickness (EWT), B) leaf structural parameter (N) or C) leaf mass per area (LMA) was varied. D) panel shows the normalized proportion of variance induced by EWT, N and LMA in these simulations.

Table 3
Statistics of linear regression models between each wavelength, measured using NIRONE S1.7 and NIRONE S2.5 sensors, and equivalent water thickness (EWT, g/m^2) and relative water content (RWC). Coefficient of determination (R^2), root-mean-square-error (RMSE) and mean absolute error (MAE) were calculated using single wavelength features ($n = 44$). Mean, maximum (max), minimum (min) and standard deviation (std) are calculated from all the developed regression model statistics.

EWT									
NIRONE S1.7 1350–1650 nm					NIRONE S2.5 2000–2450 nm				
	mean	max	min	std		mean	max	min	std
R^2	0.76	0.80	0.66	0.39	R^2	0.86	0.87	0.86	0.004
RMSE	8.0	9.48	7.29	0.63	RMSE	6.07	6.21	5.91	0.09
MAE	6.46	7.69	5.86	0.52	MAE	4.75	4.88	4.59	0.08
RWC									
NIRONE S1.7 1350–1650 nm					NIRONE S2.5 2000–2450 nm				
	mean	max	min	std		mean	max	min	std
R^2	0.77	0.80	0.73	0.02	R^2	0.81	0.82	0.79	0.007
RMSE	6.86	7.47	6.47	0.32	RMSE	6.34	6.51	6.09	0.12
MAE	5.76	6.14	5.47	0.23	MAE	5.39	5.53	5.17	0.10

Table 4
Coefficient of determination (R^2), root-mean-square-error (RMSE) and mean absolute error (MAE) for top five linear regression models for estimating equivalent water thickness (EWT, g/m^2), relative water content (RWC, %) and leaf mass per area (LMA, g/m^2) using normalized ratio index (NRI) features ($n = 44$). γ_1 and γ_2 are the reflectance of each wavelength measured by NIRONE S1.7 and NIRONE S2.5 sensors and further used to derive NRI features.

EWT									
NIRONE S1.7 1350–1650 nm					NIRONE S2.5 2000–2450 nm				
λ_1	λ_2	RMSE	R^2	MAE	λ_1	λ_2	RMSE	R^2	MAE
1390	1370	3.41	0.96	2.66	2110	2020	4.32	0.93	3.52
1390	1360	3.42	0.96	2.60	2110	2010	4.36	0.93	3.43
1380	1370	3.42	0.96	2.68	2160	2020	4.36	0.93	3.50
1390	1350	3.46	0.96	2.63	2110	2040	4.39	0.93	3.32
1380	1360	3.48	0.95	2.69	2240	2020	4.39	0.93	3.49
RWC									
NIRONE S1.7 1350–1650 nm					NIRONE S2.5 2000–2450 nm				
λ_1	$\lambda 2$	RMSE	R^2	MAE	λ_1	$\lambda 2$	RMSE	R^2	MAE
1620	1410	4.85	0.89	3.95	2160	2090	4.54	0.90	3.88
1610	1410	4.86	0.89	3.93	2160	2040	4.65	0.90	3.90
1650	1410	4.86	0.89	4.02	2160	2070	4.70	0.89	4.06
1640	1410	4.87	0.89	4.02	2160	2080	4.75	0.89	4.05
1630	1410	4.87	0.88	3.99	2160	2050	4.78	0.89	4.02
LMA									
NIRONE S1.7 1350–1650 nm					NIRONE S2.5 2000–2450 nm				
λ_1	$\lambda 2$	RMSE	R^2	MAE	λ_1	$\lambda 2$	RMSE	R^2	MAE
1650	1380	3.92	0.50	3.18	2300	2140	3.98	0.48	3.1
1530	1410	4.07	0.46	3.28	2350	2090	4.03	0.47	3.16
1600	1390	4.08	0.46	3.37	2330	2110	4.03	0.47	3.44
1640	1380	4.10	0.45	3.35	2300	2130	4.06	0.46	3.34
1560	1400	4.11	0.45	3.39	2310	2120	4.21	0.42	3.34

3.41 g/m^2. The highest estimation accuracy of RWC was achieved with NRI of wavelengths 2160 nm and 2090 nm providing an RMSE of 4.54%-units.

The NRIs also showed capabilities of predicting LMA. NRI of 1650 nm and 1380 nm wavelengths showed the highest estimation accuracy with an RMSE of 3.92 g/m^2 and a coefficient of determination of 0.5. An NRI of 2300 nm and 2140 nm wavelengths was nearly as good in predicting LMA with an RMSE of 3.98 g/m^2, explaining 48% of the variation in LMA.

3.3. Improving the prediction of relative water content using equivalent water thickness and leaf mass per area

Based on data from live trees from the field (Experiment 3), the measured leaf structural traits (EWT, LMA and RWC) were all significantly correlated ($p < 0.01$) with each other. EWT and LMA showed the highest correlation coefficient ($r = 0.91$), EWT and RWC were moderately correlated ($r = 0.68$) and the lowest correlation coefficient was found between RWC and LMA ($r = 0.46$). We also found a significant correlation between LMA and turgid weight per leaf area ($r = 0.86$) indicating a link between LMA, and the maximum water storage capacity based on the laboratory measurements (Fig. 5).

We further tested the dependencies between destructively measured leaf structural traits and found that using both EWT and LMA as explanatory variables in predicting RWC led to a significantly higher coefficient of determination ($R^2 = 0.61$) compared to using only EWT in explaining RWC ($R^2 = 0.46$) (Fig. 6).

Our findings above further indicated a link between LMA and RWC, thus, the prediction of RWC using leaf reflectance spectrum was explored using two approaches: a direct prediction using a single spectral feature for estimating RWC and an alternative approach using a combination of spectral features that were the most accurate predictors of EWT and LMA. We found that an NRI of 2160 nm and 2090 nm wavelengths (best predictor for RWC) slightly outperformed a linear

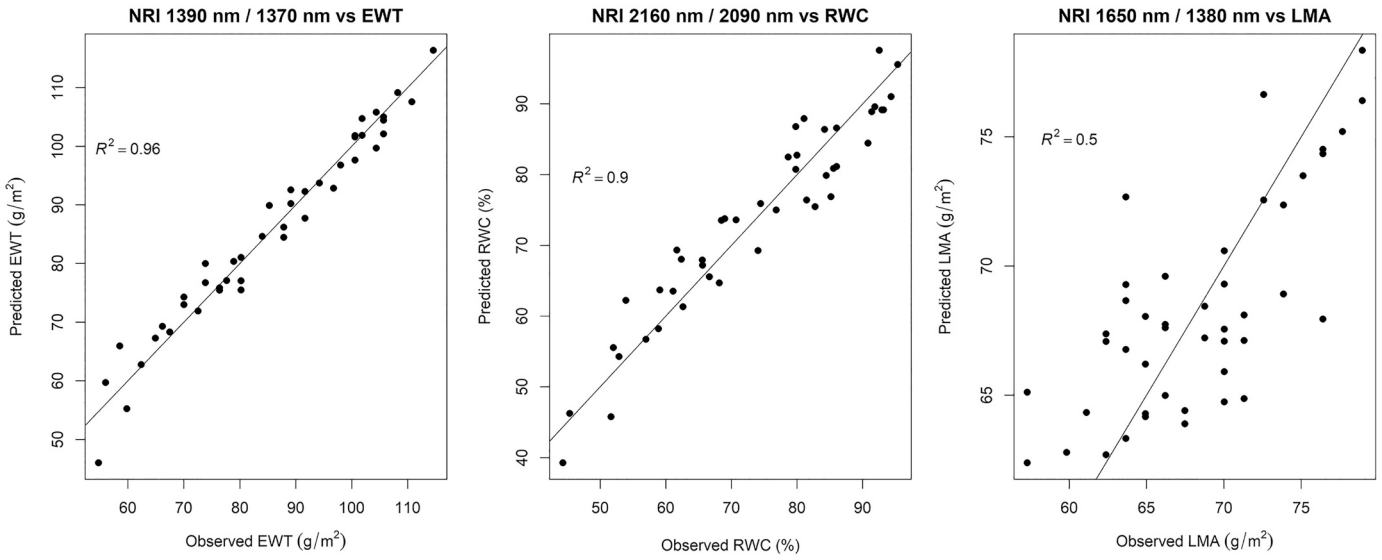

Fig. 4. Observed and predicted equivalent water thickness (EWT), relative water content (RWC) and leaf mass per area (LMA) using the regression models with normalized ratio index (NRI) features that resulted in the highest accuracy based on coefficient of determination (R^2) and root-mean-square-error. EWT was predicted using the NRI of 1390 nm and 1370 nm wavelengths, RWC was predicted using the NRI of 2160 nm and 2090 nm wavelengths and LMA was predicted using the NRI of 1650 nm and 1380 nm. The line depicts 1:1 relationship and the regression line (not visible due to non-biased estimates).

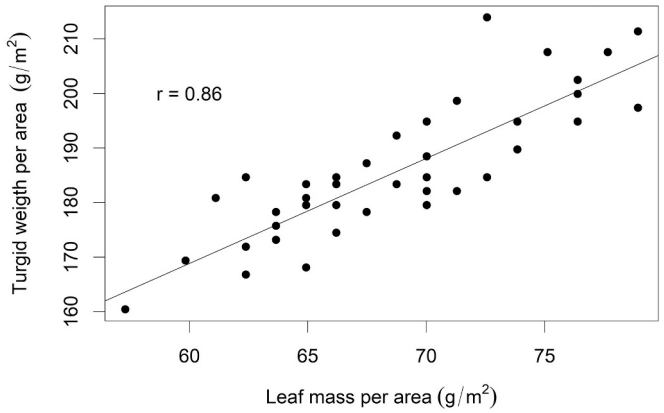

Fig. 5. The relationship between leaf mass per area (g/m^2) and turgid weight per area (g/m^2) ($n = 44$).

regression model that employed the best spectral predictors of EWT and LMA with coefficients of determination of 0.90 and 0.89, respectively (Fig. 7).

3.4. *In-situ monitoring reveals detailed diurnal leaf water content dynamics (Experiment 2)*

The NIRONE S1.7 and S2.5 sensors showed to be able to explain most of the variation in TLW ranging from 90% using single wavelengths to 99% using NRIs (Table 5) reflecting the reduction of leaf water content as drought increased. NRIs outperformed the reflectance of single wavelengths in terms of R^2. The mean of NRI using 2340 nm and 2220 nm wavelengths showed nearly 1:1 correlation with TLW, but it could be observed that the measurements of NIRONE S2.5 using the 2000–2450 nm spectral range contained much more noise than the other sensors reducing the ability to measure diurnal dynamics of leaf water content (Appendix A). However, measurements in the 1350–1650 nm spectral range showed a clear diurnal trend. Visualization of the top NRIs in predicting TLW revealed that NRIs that employed neighboring wavelengths (e.g., 1540 nm and 1530 nm) contained more noise in the signal compared to NRIs (see Appendix A), which used wavelengths further apart (e.g., 1470 nm and 1350 nm). Thus, the NRI of 1470 nm and 1350 nm was used for predicting diurnal changes in RWC for *D. marginate*.

After identifying suitable wavelengths for *D. marginate*, a linear regression model using the measurements of experiment 1 was used to create a linear regression model for predicting changes in RWC. Fig. 7 shows that according to the prediction, RWC varied between 79% and 83% during the monitoring period with declining RWC as drought intensified and TLW increased. It could be observed that the diurnal variation of predicted RWC was affected by both air temperature, as changes in air temperature mainly control the evaporative demand due to its effect on VPD, and TLW. The amplitude of RWC variation was greater in well-watered conditions and reduced as time from last watering increased (Fig. 8). It is also observable how RWC maintains a higher level after watering for four or five days before it begun to gradually reduce towards the end of the drought period.

3.5. *Time-series of hyperspectral imaging can capture diurnal leaf water dynamics (Experiment 3)*

The results of Experiment 1 were utilized to estimate diurnal variation in RWC of silver birch in field conditions using repeated measurements. We estimated RWC using a direct approach by utilizing the NRI of 1620 nm and 1410 nm wavelengths and using an alternative approach through the prediction of EWT and LMA with NRIs of 1390 nm and 1370 nm (EWT predictor) and 1650 nm and 1380 nm (LMA predictor) wavelengths (Fig. 9). Direct RWC estimation explained 70% of the variation in destructively measured RWC during the monitoring period. The regression model explained 81% of the variation in RWC when EWT and LMA were employed as predictors.

However, the direct estimation of RWC with the NRI of 1620 nm and 1410 nm wavelengths seemed to produce more constant RWC estimates on the leaf-level through the measurement period (Fig. 10). The direct estimation of RWC produced estimates that correspond well with destructively measured RWC in terms of both the diurnal trend and the predicted values. The changes in RWC also correspond well with the diurnal pattern of VPD. The estimation of RWC through spectral features of EWT and LMA did not produce as consistent diurnal patterns of RWC as the direct estimation of RWC did, but differences between individual leaves were greater.

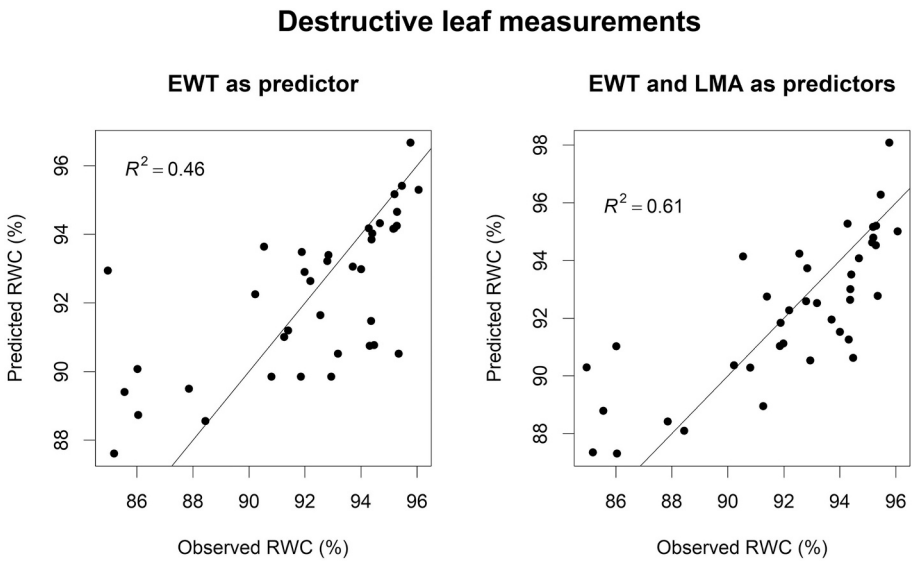

Fig. 6. Observed and predicted relative water content (RWC) using equivalent water thickness and leaf mass per area using destructive leaf measurements as predictors in linear regression modelling ($n = 39$). The line depicts 1:1 relationship.

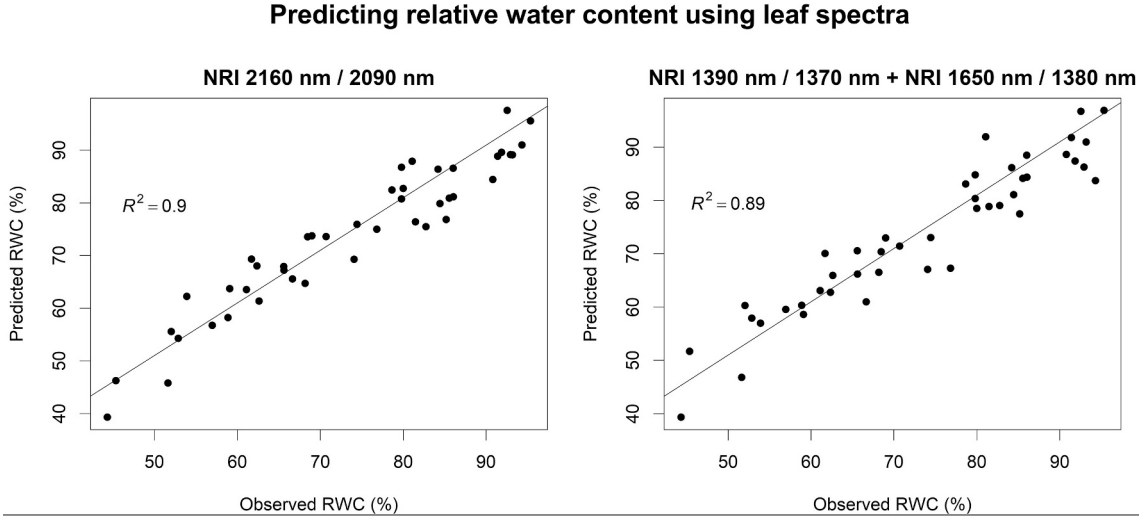

Fig. 7. Direct approach in prediction of relative water content (RWC) using a normalized ratio index (NRI) of 2160 nm and 2090 nm wavelengths and an alternative approach using a combination of NRIs of 1390 nm and 1370 nm wavelengths (best predictor of equivalent water thickness) and 1650 nm and 1380 nm wavelengths (best predictor of leaf mass per area). The line depicts 1:1 relationship and the regression line (not visible due to non-biased estimates).

4. Discussion

In this study, we aimed to demonstrate the capabilities of hyperspectral spectroscopy in measuring timely changes in leaf water content. We showed that low-cost hyperspectral sensors can be used to monitor changes in leaf water content that occur in a diurnal fashion.

We found strong linear relationships between the measured spectra, the spectral features, and leaf water content measured both as EWT and RWC, in our laboratory experiment (Experiment 1). A slightly higher accuracy was achieved in estimating EWT than RWC and there were differences in the wavelengths that provided these estimates. EWT was estimated best with a narrow spectral region using spectral features between 1350 nm and 1390 nm, but longer wavelengths resulted in the most reliable RWC estimates with an NRI of 1620 nm and 1410 nm and NRI of 2160 nm and 2090 nm wavelengths. Our simulation results supported the experimental findings. The 1620 nm and 1410 nm wavelengths are located in regions that show higher proportion of variance induced by LMA and EWT in the SWIR region, respectively, likely resulting in better prediction of RWC. Similar results in the estimation of EWT and RWC have been obtained many times before in several studies, showcasing various techniques that can be used to estimate leaf water content (Cheng et al., 2011; Feret et al., 2011). The spectral features showed also capabilities in explaining up to 50% of variation in LMA using an NRI of 1650 nm and 1380 nm wavelengths. The purpose of the first experiment was to validate the well-known relationships between leaf water content and the spectral features, to give an estimate of the accuracy of the used method in estimating EWT, RWC and LMA and to identify suitable wavelengths for estimating them for silver birch.

4.1. The role of leaf mass per area in predicting relative water content

Interrelations of EWT, RWC and LMA were investigated using the leaf measurements of Experiments 1 and 3 to explore the role of LMA in predicting RWC. A significantly larger proportion of variation in RWC could be explained using both EWT and LMA as predictors of RWC

Table 5
Coefficient of determination (R^2) for the top five regression models between time from last watering (TLW) and daily metrics of spectral features for each sensor. The monitoring period lasted 12 days. γ_1 and γ_2 are the reflectance of each wavelength used in normalized ratio index calculations.

NIRONE S1.7 1350–1650 nm						
NRI (λ_1, λ_2)				Reflectance at λ		
λ_1	λ_2	R^2	feature	λ	R^2	feature
1540	1530	0.91	mean	1460	0.76	range
1420	1400	0.90	mean	1450	0.75	range
1410	1400	0.88	mean	1470	0.74	range
1470	1350	0.87	mean	1370	0.74	range
1550	1530	0.87	mean	1360	0.72	range
NIRONE S2.5 2000–2450 nm						
NRI (λ_1, λ_2)				Reflectance at λ		
λ_1	λ_2	R^2	feature	λ	R^2	feature
2340	2220	0.99	mean	2450	0.90	mean
2330	2260	0.99	mean	2440	0.88	mean
2340	2310	0.99	range	2430	0.85	mean
2330	2270	0.99	mean	2420	0.83	mean
2320	2260	0.99	mean	2410	0.80	mean

compared to using EWT only indicating that LMA estimation could improve estimates of RWC. The prediction of RWC using spectral features was investigated using a direct approach (the best estimator of RWC) and through a combination of spectral features estimating EWT and LMA. Both approaches yielded similar results in the laboratory setting in Experiment 1, but the direct approach seemed to produce more consistent results in the field (Experiment 3). The direct estimation of RWC yielded results that were well aligned with the diurnal trend of destructively measured RWC. This could be a result of increased measurement noise when utilizing two spectral features that are close to each other simultaneously in the EWT-LMA approach.

The role of LMA in predicting RWC is likely to increase when a larger range of different leaf structures and species are measured. However, it may be that a general model that can accurately capture variation in RWC is not achievable, but local and species-wise models are needed for the accurate estimation of RWC from leaf spectral information.

4.2. Monitoring of diurnal variation in leaf water content

The second experiment demonstrated continuous in-situ monitoring of leaf spectra and leaf water content. Suitable wavelengths were investigated with regression modelling between TLW and spectral features to identify suitable wavelengths for *D. marginate* and RWC was predicted through the monitoring period. The diurnal dynamics of leaf water content were clearly observable in the leaf spectra with spectral features from the 1350–1650 nm region (Fig. 8), but the 2000–2450 nm spectral region (NIRONE S2.5) did not show a clear diurnal trend due to a high amount of noise in the measurement (see Appendix A). It could be observed from the time-series of predicted RWC (Fig. 8) how the amplitude of diurnal RWC decreases as drought develops and is restored after the plant is watered. The range of predicted RWC was 79%–83% where the highest values were for a rewatered plant indicating unrealistic values of RWC (well-watered plants should have a RWC of ~95%) (Mullan and Pietragalla, 2012). The predicted RWC was likely biased due to the utilization of measurements from a different species (silver birch) in model development, which might also include some oversaturation issues of RWC explained in the methods of experiment 1.

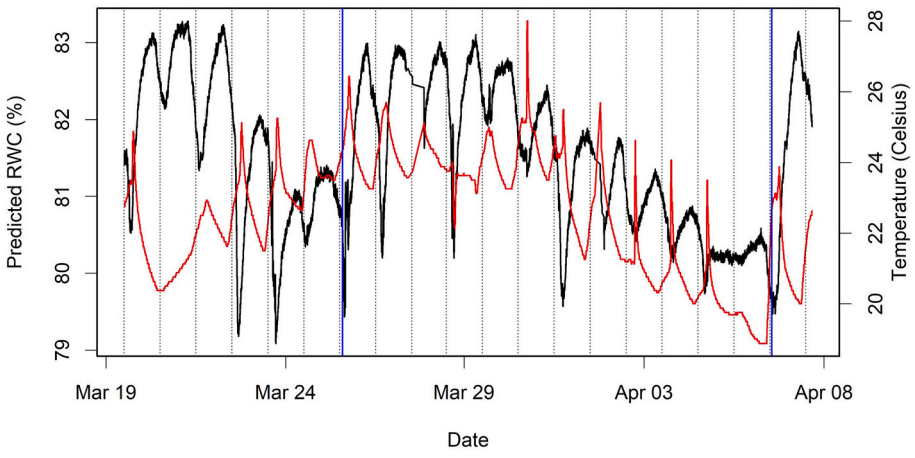

Fig. 8. Predicted relative water content (RWC) using the moving average of 20 reflectance measurements of normalized ratio index (NRI) of 1470 nm and 1350 nm wavelengths (black line) and air temperature (red line) during the monitoring period (March 19–April 8) of a *Dracaena marginate* (Lem.) leaf. Blue vertical lines denote a watering. The reflectance measurements were conducted every 48 s and temperature measurements every 15 min. Dashed lines denote the midday (12:00) of each day. (For interpretation of the references to colour in this figure legend, the reader is referred to the web version of this article.)

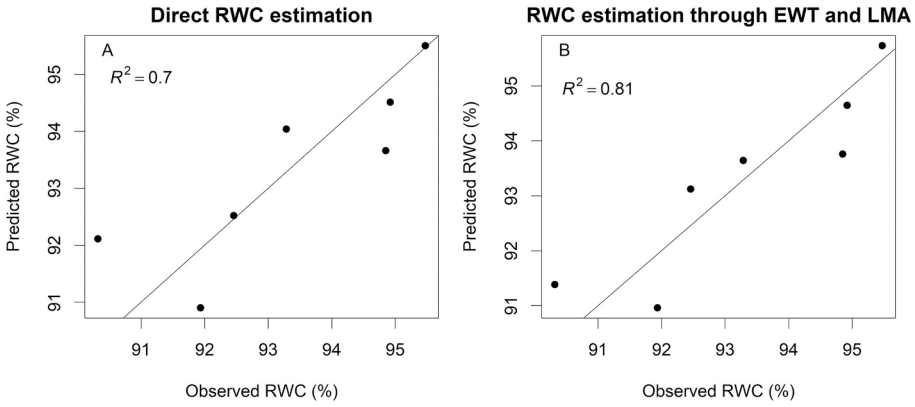

Fig. 9. Linear regression models between observed (destructively measured, $n = 21$) and predicted relative water content (RWC, $n = 70$) using A) direct estimation with a normalized ratio index (NRI) of 1620 nm and 1410 nm wavelengths and B) estimation through equivalent water thickness (EWT) and leaf mass per area (LMA) using NRIs of 1390 nm and 1370 nm (predictor for EWT) and 1650 nm and 1380 nm (predictor for LMA) wavelengths. The line represents the 1:1 ratio and the regression line (lines too close to each other to be visible).

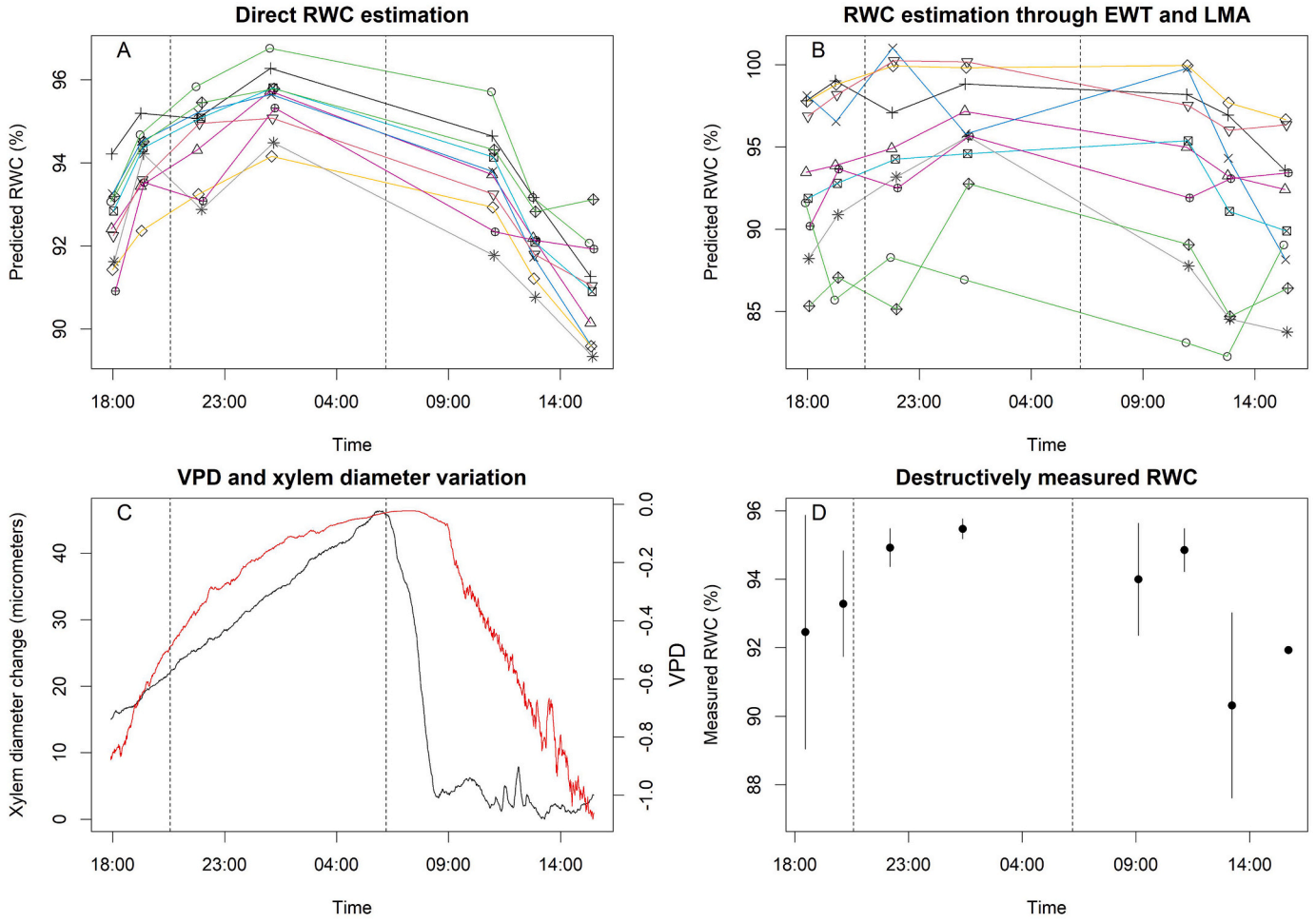

Fig. 10. A) Relative water content (RWC) estimated using a normalized ratio index (NRI) of 1620 nm and 1410 nm wavelengths. Individual leaves are plotted with different colors. B) RWC estimated using NRIs of 1390 nm and 1370 nm (predictor for equivalent water thickness, EWT) and 1650 nm and 1380 nm (predictor for leaf mass per area, LMA) wavelengths. C) Variation in vapour pressure deficit (VPD, the red line) and xylem diameter (black line) during the monitoring period. D) Destructively measured RWC during the monitoring period. The error bars represent standard deviation from the mean. The dashed vertical lines denote sunset and sunrise. (For interpretation of the references to colour in this figure legend, the reader is referred to the web version of this article.)

However, these issues are only circumstantial as the goal was to investigate if our sensor can observe the diurnal fluctuations in leaf water content, which were clearly observable in the measurements. The issues mentioned here were not apparent in Experiment 3, where the more robust standing method was used for measuring RWC and the same species was used for model development and predictions. The signal-to-noise ratio of the NIRONE S2.5 sensor (1500 vs. 11,000 in S1.7) seemed to hamper the measurement of diurnal dynamics despite the high correlation between TLW and spectral features and the high sensitivity to leaf water content (Feret et al., 2019). Therefore, the NIRONE sensor S1.7 seems like a more viable option for continuous measurement of leaf water content.

The daily dynamics that were observed in the *D. marginate* leaves correspond well with previous measurements of diurnal sap flow and xylem diameter dynamics in drought conditions (Jupa et al., 2017). We could observe in our measurements that the amplitude of variation was decreasing towards more severe drought conditions and that the amplitude of variation returned after watering similarly to the observations made by Jupa et al. (2017). Although it is challenging to fully understand the magnitude of changes in water content and convert the observed values in reflectance to absolute amounts of water, we can use this type of data to understand the variability of leaf water content. There is also a vast body of literature that supports our findings of the sensitivity of the investigated spectral regions on leaf water content (Cheng et al., 2011; Feret et al., 2008; Romer et al., 2012). We already have a detailed understanding of the physical changes of water on electromagnetic radiation and the relationship between water content and SWIR radiation (Becker and Autler, 1946; Lunkenheimer et al., 2017), but the lack of suitable and affordable instruments has been hampering the full application of this knowledge.

Based on our results, a spectral region in the 1350–1470 nm range showed to be especially important for the estimation of leaf water content and information on leaf structure and LMA was more focused in the 1600–1650 nm range. This indicates that narrow spectral ranges or measured wavelengths could capture changes in the investigated variables. The NIRONE sensors are programmable, and the measured wavelengths can be selected. This feature allows more rapid measurements to be undertaken when the number of measured wavelengths is lowered enabling ultra-high time resolutions in measuring leaf spectra if needed.

We observed that the measurement setup is very sensitive to any changes in viewing angle and distance on the measured spectra (not reported). Therefore, we suggest that to measure the daily changes of leaf water content, the sensor needs to be carefully installed and care taken so that the leaf does not change position during the measurement period and does not cause alteration to the measured reflectance due to changes in bidirectional reflectance distribution function. The sensor also causes a small heating effect as the lamp illuminates the target,

which could lead to bias during long-term monitoring on estimated leaf water content variation if VPD increases between the leaf and the sensor. Higher VPD could lead to increased transpiration and thus, also to a smaller leaf water content. However, no visible damage or effect on the measured leaves was observed during or after the 20-day monitoring period.

The purpose of the third experiment was to test the sensors in a forest field experiment with mature silver birch trees and to measure diurnal dynamics of leaf water content in the field. Our results show that distinct diurnal trends of RWC were captured using a direct approach for estimating RWC with an NRI of 1620 nm and 1410 nm wavelengths, which corresponded well with the trend in destructively measured RWC and VPD (Fig. 10). Different leaves showed varying ranges of RWC that may be due to differences in leaf structure (described with leaf structural parameter N), which the spectral feature is not capable of taking into account. We also used spectral features that predicted EWT (NRI of 1370 nm and 1390 nm) and LMA (NRI of 1650 nm and 1380 nm) to estimate RWC, which resulted in a better relationship (R^2 of 0.81 vs. 0.7) with measured RWC when the measurements were averaged. However, the leaf-level predictions of RWC using the EWT-LMA approach showed larger variability and inconsistencies when compared to the trend in measured RWC during the monitoring period, which could be a result of increased noise due to the utilization of an additional spectral feature.

The measurements of the third experiment were conducted using only single measurements aiming at avoiding the change of exact measurement position between different measurements. This could have affected the results, because of possible variation in the measurements and it could be more advisable to use many measurements of a single leaf. Afterall, the measurement area of the NIRONE sensor is tiny, about a millimeter in diameter, and the viewing angle is very narrow, only about 8 degrees. Therefore, multiple measurements of each leaf could give a more stable measurement of the leaf spectra, which can be influenced also by varying leaf water content within the leaf.

A disadvantage of the presented method is the lack of multiple pixels compared to other imaging sensors, such as terahertz radiation spectroscopy (Browne et al., 2020) or terrestrial lidar (Elsherif et al., 2019b; Junttila et al., 2021). Spatial variation of leaf water content is more difficult to measure using the presented method, but on the other hand we were able to observe very clearly the small diurnal variation in leaf water content, which has been difficult to measure non-destructively. An interesting future approach would be to combine a time-series of hyperspectral spectroscopy at leaf-level and use that to up-scale the measurements to canopy-level using terrestrial lidar.

5. Conclusions

The results of this study showcase how low-cost (under 2500 €) hyperspectral spectroscopy can be used to estimate EWT and RWC and assess detailed leaf water content dynamics through time. The NIRONE sensors seem to embody spectral resolution and accuracy that enables the monitoring of leaf spectra in the SWIR region at a reasonable cost allowing multiple prominent applications for monitoring leaf water content. According to the results, the estimation of RWC through the estimation of EWT and LMA may improve estimation accuracy. However, a direct estimation of RWC from leaf spectra yielded better results in this study. Based on our results, the spectral region between 1350 nm and 1650 nm can be used to estimate EWT, RWC and LMA. Detailed temporal monitoring of leaf water dynamics can help us to further understand the movement of water within the soil-tree-atmosphere continuum. These low-cost sensors open new avenues for research in studying plant-water interactions by allowing continuous measurements and the detection of minute changes in leaf water content.

Credit author statement

Samuli Junttila contributed to study conceptualization, data curation, formal analysis, funding acquisition and wrote the original draft of the manuscript. Teemu Hölttä contributed to study conceptualization, resources and writing of the original draft of the manuscript. Ninni Saarinen contributed to formal analysis and reviewing the manuscript. Ville Kankare, Tuomas Yrttimaa and Juha Hyyppä contributed to resources and participated in reviewing and editing of the manuscript. Mikko Vastaranta participated in writing the original draft and to reviewing and editing of the manuscript and to study conceptualization. All authors have read and approved the manuscript.

Declaration of Competing Interest

None.

Acknowledgements

The research was funded by the Academy of Finland [grant numbers 330422, 315079, 345166, 337656, 337811 and 337810]. This study has been done with affiliation to the Academy of Finland Flagship Forest-Human-Machine Interplay - Building Resilience, Redefining Value Networks and Enabling Meaningful Experiences (UNITE) [grant number 337127].

Appendix A. Appendix

The appendix contains two figures from the Experiment 2 showing the increases in noise when NIRONE S2.5 was used for measuring leaf spectra (Fig. A1) and when neighboring bands were used for calculating NRI (Fig. A2).

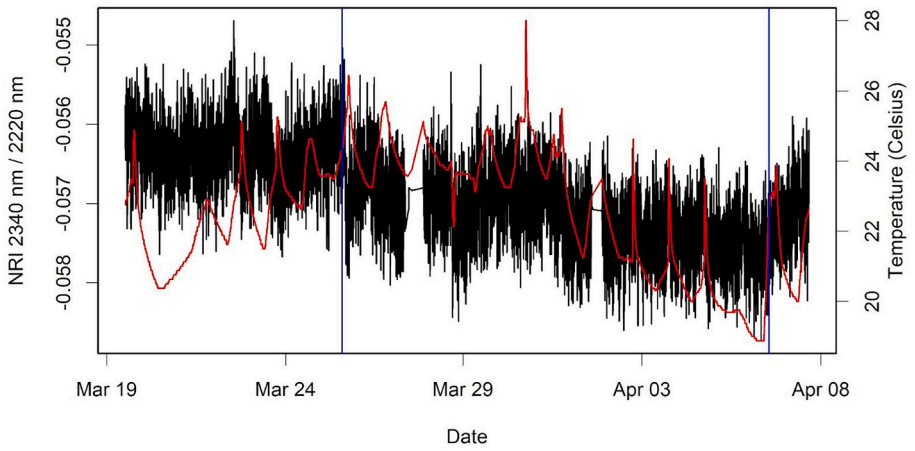

Fig. A1. Moving average of 10 measurements of normalized ratio index (NRI) of 2340 nm and 2220 nm wavelengths (black line) of a *Dracaena marginate* (Lem.) leaf and air temperature (red line) during the monitoring period (March 19–April 8). The vertical blue lines denote the timing of watering. The reflectance measurements were conducted every 48 s and temperature measurements every 15 min. (For interpretation of the references to colour in this figure legend, the reader is referred to the web version of this article.)

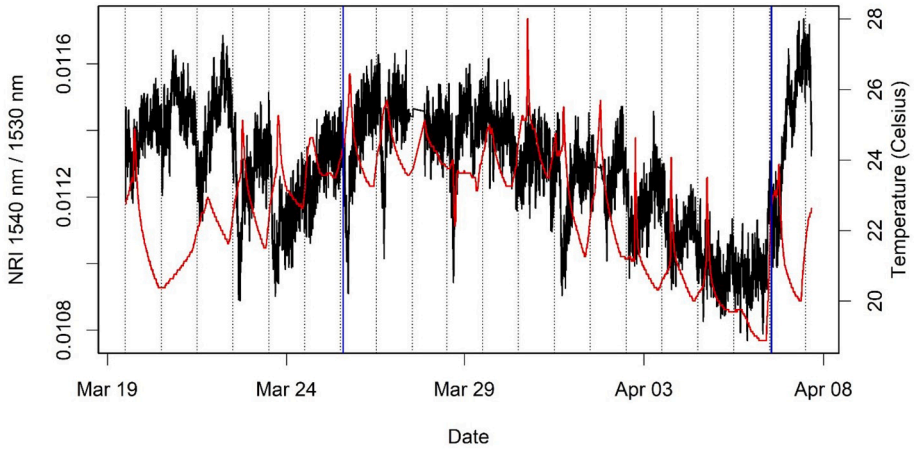

Fig. A2. Moving average of 10 measurements of normalized ratio index (NRI) of 1540 nm and 1530 nm wavelengths (black line) of a *Dracaena marginate* (Lem.) leaf and air temperature (red line) during the monitoring period (March 19–April 8). The vertical blue lines denote the timing of watering. The reflectance measurements were conducted every 48 s and temperature measurements every 15 min. (For interpretation of the references to colour in this figure legend, the reader is referred to the web version of this article.)

Appendix B. Supplementary data

Supplementary data to this article can be found online at https://doi.org/10.1016/j.rse.2022.113071.

References

Arndt, S.K., Irawan, A., Sanders, G.J., 2015. Apoplastic water fraction and rehydration techniques introduce significant errors in measurements of relative water content and osmotic potential in plant leaves. Physiol. Plant. 155, 355–368.

Bartlett, M.K., Scoffoni, C., Sack, L., 2012. The determinants of leaf turgor loss point and prediction of drought tolerance of species and biomes: a global meta-analysis. Ecol. Lett. 15, 393–405.

Beć, K.B., Grabska, J., Siesler, H.W., Huck, C.W., 2020. Handheld near-infrared spectrometers: where are we heading? NIR News 31, 28–35.

Becker, G.E., Autler, S.H., 1946. Water vapor absorption of electromagnetic radiation in the centimeter wave-length range. Phys. Rev. 70, 300.

Boren, E.J., Boschetti, L., Johnson, D.M., 2019. Characterizing the variability of the structure parameter in the PROSPECT leaf optical properties model. Remote Sens. 11, 1236.

Browne, M., Yardimci, N.T., Scoffoni, C., Jarrahi, M., Sack, L., 2020. Prediction of leaf water potential and relative water content using terahertz radiation spectroscopy. Plant Direct 4, e00197.

Buckley, T.N., 2005. The control of stomata by water balance. New Phytol. 168, 275–292.

Campany, C.E., Tjoelker, M.G., von Caemmerer, S., Duursma, R.A., 2016. Coupled response of stomatal and mesophyll conductance to light enhances photosynthesis of shade leaves under sunflecks. Plant Cell Environ. 39, 2762–2773.

Ceccato, P., Flasse, S., Tarantola, S., Jacquemoud, S., Gregoire, J.M., 2001. Detecting vegetation leaf water content using reflectance in the optical domain. Remote Sens. Environ. 77, 22–33.

Cheng, T., Rivard, B., Sanchez-Azofeifa, A., 2011. Spectroscopic determination of leaf water content using continuous wavelet analysis. Remote Sens. Environ. 115, 659–670.

Danson, F.M., Steven, M.D., Malthus, T.J., Clark, J.A., 1992. High-spectral resolution data for determining leaf water-content. Int. J. Remote Sens. 13, 461–470.

Dewar, R., Mauranen, A., Mäkelä, A., Hölttä, T., Medlyn, B., Vesala, T., 2018. New insights into the covariation of stomatal, mesophyll and hydraulic conductances from optimization models incorporating nonstomatal limitations to photosynthesis. New Phytol. 217, 571–585.

Egilla, J.N., Davies, F.T., Boutton, T.W., 2005. Drought stress influences leaf water content, photosynthesis, and water-use efficiency of Hibiscus rosa-sinensis at three potassium concentrations. Photosynthetica 43, 135–140.

Elsherif, A., Gaulton, R., Mills, J., 2019a. Four dimensional mapping of vegetation moisture content using dual-wavelength terrestrial laser scanning. Remote Sens. 11, 2311.

Elsherif, A., Gaulton, R., Shenkin, A., Malhi, Y., Mills, J., 2019b. Three dimensional mapping of forest canopy equivalent water thickness using dual-wavelength terrestrial laser scanning. Agric. For. Meteorol. 276, 107627.

Feret, J.B., Francois, C., Asner, G.P., Gitelson, A.A., Martin, R.E., Bidel, L.P.R., Ustin, S.L., le Maire, G., Jacquemoud, S., 2008. PROSPECT-4 and 5: advances in the leaf optical

properties model separating photosynthetic pigments. Remote Sens. Environ. 112, 3030–3043.
Feret, J.B., Francois, C., Gitelson, A., Asner, G.P., Barry, K.M., Panigada, C., Richardson, A.D., Jacquemoud, S., 2011. Optimizing spectral indices and chemometric analysis of leaf chemical properties using radiative transfer modeling. Remote Sens. Environ. 115, 2742–2750.
Féret, J.-B., Gitelson, A., Noble, S., Jacquemoud, S., 2017. PROSPECT-D: towards modeling leaf optical properties through a complete lifecycle. Remote Sens. Environ. 193, 204–215.
Feret, J.B., le Maire, G., Jay, S., Berveiller, D., Bendoula, R., Hmimina, G., Cheraiet, A., Oliveira, J.C., Ponzoni, F.J., Solanki, T., de Boissieu, F., Chave, J., Nouvellon, Y., Porcar-Castell, A., Proisy, C., Soudani, K., Gastellu-Etchegorry, J.P., Lefevre-Fonollosa, M.J., 2019. Estimating leaf mass per area and equivalent water thickness based on leaf optical properties: potential and limitations of physical modeling and machine learning. Remote Sens. Environ. 231, 110959.
Garnier, E., Laurent, G., 1994. Leaf anatomy, specific mass and water content in congeneric annual and perennial grass species. New Phytol. 128, 725–736.
Hao, G.Y., Sack, L., Wang, A.Y., Cao, K.F., Goldstein, G., 2010. Differentiation of leaf water flux and drought tolerance traits in hemiepiphytic and non-hemiepiphytic Ficus tree species. Funct. Ecol. 24, 731–740.
Huck, C.W., 2021. New trend in instrumentation of NIR spectroscopy—miniaturization. In: Near-Infrared Spectroscopy. Springer, pp. 193–210.
Junttila, S., Holopainen, M., Vastaranta, M., Lyytikäinen-Saarenmaa, P., Kaartinen, H., Hyyppä, J., Hyyppä, H., 2019. The potential of dual-wavelength terrestrial lidar in early detection of Ips typographus (L.) infestation–leaf water content as a proxy. Remote Sens. Environ. 231, 111264.
Junttila, S., Hölttä, T., Puttonen, E., Katoh, M., Vastaranta, M., Kaartinen, H., Holopainen, M., Hyyppä, H., 2021. Terrestrial laser scanning intensity captures diurnal variation in leaf water potential. Remote Sens. Environ. 255, 112274.
Jupa, R., Plichta, R., Paschová, Z., Nadezhdina, N., Gebauer, R., 2017. Mechanisms underlying the long-term survival of the monocot Dracaena marginata under drought conditions. Tree Physiol. 37, 1182–1197.
Konings, A.G., Rao, K., Steele-Dunne, S.C., 2019. Macro to micro: microwave remote sensing of plant water content for physiology and ecology. New Phytol. 223, 1166–1172.
Korpela, I., 2017. Acquisition and evaluation of radiometrically comparable multi-footprint airborne LiDAR data for forest remote sensing. Remote Sens. Environ. 194, 414–423.
Kotz, B., Schaepman, M., Morsdorf, F., Bowyer, P., Itten, K., Allgower, B., 2004. Radiative transfer modeling within a heterogeneous canopy for estimation of forest fire fuel properties. Remote Sens. Environ. 92, 332–344.
Lehnert, L.W., Meyer, H., Obermeier, W.A., Silva, B., Regeling, B., Bendix, J., 2018. Hyperspectral Data Analysis in R: The Hsdar Package arXiv preprint arXiv: 1805.05090.
Li-Ping, B., Fang-Gong, S., Ti-Da, G., Zhao-Hui, S., Yin-Yan, L., Guang-Sheng, Z., 2006. Effect of soil drought stress on leaf water status, membrane permeability and enzymatic antioxidant system of maize. Pedosphere 16, 326–332.
Lunkenheimer, P., Emmert, S., Gulich, R., Köhler, M., Wolf, M., Schwab, M., Loidl, A., 2017. Electromagnetic-radiation absorption by water. Phys. Rev. E 96, 062607.
Mullan, D., Pietragalla, J., 2012. Leaf relative water content. In: Physiological breeding II: A Field Guide to Wheat Phenotyping, pp. 25–27.
Penuelas, J., Filella, I., Biel, C., Serrano, L., Save, R., 1993. The reflectance at the 950–970 nm region as an indicator of plant water status. Int. J. Remote Sens. 14, 1887–1905.
Penuelas, J., Pinol, J., Ogaya, R., Filella, I., 1997. Estimation of plant water concentration by the reflectance water index WI (R900/R970). Int. J. Remote Sens. 18, 2869–2875.
Rahimi, A., Hosseini, S.M., Pooryoosef, M., Fateh, I., 2010. Variation of leaf water potential, relative water content and SPAD under gradual drought stress and stress recovery in two medicinal species of Plantago ovata and P. psyllium. Plant Ecophysiol. 2, 53–60.
Romer, C., Wahabzada, M., Ballvora, A., Pinto, F., Rossini, M., Panigada, C., Behmann, J., Leon, J., Thurau, C., Bauckhage, C., Kersting, K., Rascher, U., Plumer, L., 2012. Early drought stress detection in cereals: simplex volume maximisation for hyperspectral image analysis. Funct. Plant Biol. 39, 878–890.
Rosas, T., Mencuccini, M., Barba, J., Cochard, H., Saura-Mas, S., Martínez-Vilalta, J., 2019. Adjustments and coordination of hydraulic, leaf and stem traits along a water availability gradient. New Phytol. 223, 632–646.
Schymanski, S.J., Or, D., Zwieniecki, M., 2013. Stomatal control and leaf thermal and hydraulic capacitances under rapid environmental fluctuations. PLoS One 8, e54231.
Sperry, J.S., Wang, Y., Wolfe, B.T., Mackay, D.S., Anderegg, W.R., McDowell, N.G., Pockman, W.T., 2016. Pragmatic hydraulic theory predicts stomatal responses to climatic water deficits. New Phytol. 212, 577–589.
Tucker, C.J., 1980. Remote sensing of leaf water content in the near infrared. Remote Sens. Environ. 10, 23–32.
Turner, N., Long, M., 1980. Errors arising from rapid water loss in the measurement of leaf water potential by the pressure chamber technique. Funct. Plant Biol. 7, 527–537.
Tuzet, A., Perrier, A., Leuning, R., 2003. A coupled model of stomatal conductance, photosynthesis and transpiration. Plant Cell Environ. 26, 1097–1116.
White, D., Beadle, C., Worledge, D., 1996. Leaf water relations of Eucalyptus globulus ssp. globulus and E. nitens: seasonal, drought and species effects. Tree Physiol. 16, 469–476.
Yang, J., Yang, S., Zhang, Y., Shi, S., Du, L., 2021. Improving characteristic band selection in leaf biochemical property estimation considering interrelations among biochemical parameters based on the PROSPECT-D model. Opt. Express 29, 400–414.